Applied Mechanics and Materials *Online: 2014-02-27*
ISSN: 1662-7482, Vols. 530-531, pp 7-14
doi:10.4028/www.scientific.net/AMM.530-531.7

A Novel RFID-Based Thermal Convection Inclinometer on Flexible Substrate without Grooved Structure

Jium-Ming Lin[1, a], Cheng-Hung Lin[2,b] and Chia-Hsien Lin[3,c]

[1]Department of Communication Engineering, Chung-Hua University, Hsin-Chu, Taiwan 30012

[2]Ph. D. Program in Eng. Science College of Eng., Chung-Hua University, Hsin-Chu, Taiwan 30012

[3]Department of Electrical Engineering, Chung-Hua University, Hsin-Chu, Taiwan 30012

[a]jmlin@chu.edu.tw, [b]b09306014@chu.edu.tw, [c]bibby790204@yahoo.com.tw

Keywords: Inclinometer, flexible substrate, hemi-spherical shape, non-floating structure, thermal convection, RFID-based.

Abstract. This research proposes a novel wireless RFID-based thermal convection type inclinometer by using non-floating structure without a cavity in the substrate. Four new ideas are presented. The first one is to make the device on a flexible substrate, thus it can save more energy than the traditional silicon. The second one is to integrate both an inclinometer and a wireless RFID antenna on the same substrate, such that it is a wireless device and very convenient for usage. The third idea is to fill xenon gas in the chamber with hemi-spherical or hemi-cylindrical shape instead of the previous one with carbon dioxide and rectangular shape. Because the xenon gas would not produce oxidization effect to the heater, so it would be more reliable. The fourth idea is to use non-floating structure instead of the floating one. The results by using floating structure with xenon and CO_2 gases are studied the first; but the sensitivity performances are not good. Note that the sensitivities for the proposed non-floating structure by using hemi-spherical chamber filled with xenon and CO_2 gases are better, and the one of the former is better than the latter by 70 %. On the other hand, the response speed (step-input of tilted angle) by using hemi-cylindrical chamber with xenon gas is the quickest, the average response time is 545μs, while the rectangular chamber filled with CO_2 is the slowest, and the average response time is 848μs.

Introduction

The conventional inclinometers are manufactured on silicon wafers [1-22], and the chamber is filled with air or carbon dioxide [12]. However, the air and carbon dioxide contain oxygen, which may oxidize the heaters to reduce the lifespan. The key technology of this paper is to integrate both a thermal convection type inclinometer and a wireless RFID antenna on the same flexible substrate as in Fig. 1, such that the energy loss by the traditional silicon substrate can be reduced [16-17] and it is very convenient for usage. In this paper we use xenon inert gas in the chamber without oxidizing the heater as the traditional air or carbon dioxide [16-17]. Besides, the inner shape of the chamber is changed as a hemispheric or a hemi-cylindrical one instead of the rectangular type [1-22]. The results by using floating structure with xenon and CO_2 gases are studied the first; but the sensitivity curves are not good. Note that the sensitivity and response time (step-input of tilted angle) for the proposed non-floating structure by using hemispherical chamber filled with xenon and CO_2 gases are better, and the one with xenon is better than using CO_2 by 70%. The response speed (step-input of tilted angle) by using hemi-cylindrical chamber filled with xenon gas is the quickest, the average response time is 545μs, while the rectangular chamber filled with CO_2 is the slowest, and the average response time is 848μs. The paper organization is as follows: the first section is the introduction. The second one is fabrication steps. The third one is the simulation and discussion. The last part is the summary.

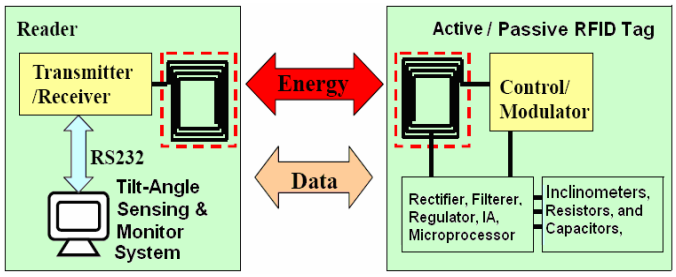

Fig.1 Block diagram of the RFID-based thermal convection type inclinometer

Fabrication steps

Step 1: Deposit SiO_2 on both sides of substrate for thermal, electrical and humidity isolation. The next is to cover Photo Resist (PR) on both sides to protect the layers of SiO_2. Cover a layer of SU-8 PR at the front side. Then using mask #1 and Photolithography And Etching Processes (PAEP), a grooved structure is formed on the substrate. The result is in Fig. 2.

Step 2: Deposit SiO_2 on the front side of substrate as the sacrificial layer; the thickness is about one half of the SU-8 layer. The next is to cover a layer of PR on the front side. Using mask #1 and PAEP, the PR on the grooved structure is remained to protect the under lying layer of SiO_2. Then remove the layer of SiO_2 around the cavity. The result is as shown in Fig. 3.

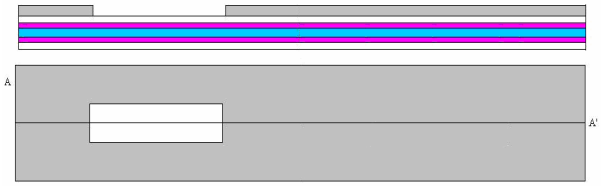

Fig. 2 Result of design Step 1

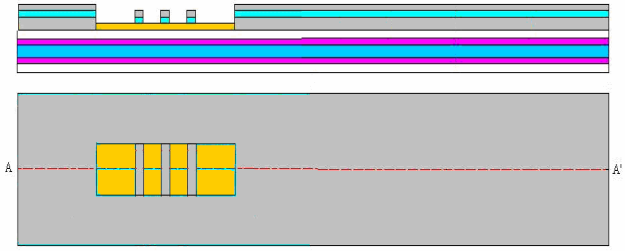

Fig. 3 Result of design Step 2

Step 3: Remove PR on the grooved structure. Deposit a layer of alumina oxide to support the heater and temperature sensors. Cover a layer of PR, and using mask #2 and PAEP, only remain the PR on the grooved structure to protect the under lying layer of alumina oxide. The result is in Fig. 4.

Step 4: Deposit a layer of p-type amorphous silicon with thickness 100-250μm, use an Nd-YAG laser to anneal it as a poly-silicon thermister. Use mask #2 and PAEP to retain the PR on the poly-silicon thermister. Finally, use KOH solution or RIE process to remove the layers of poly-silicon without PR protection. After remove the PR, the result is as shown in Fig. 5.

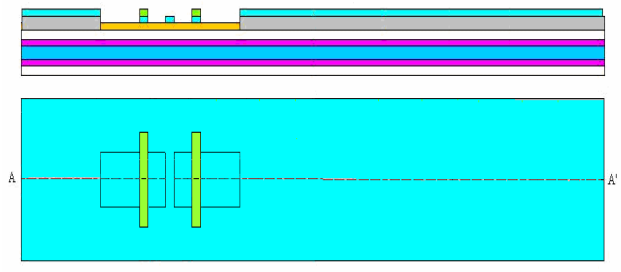

Fig. 4 Result of design Step 3

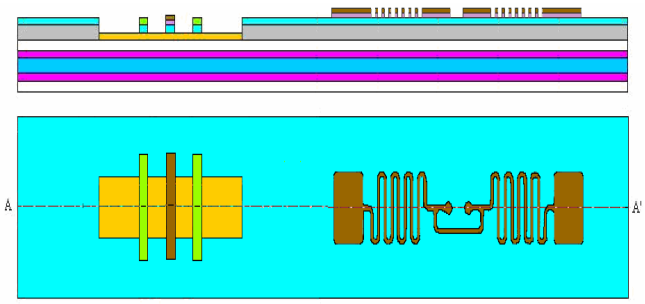

Fig. 5 Result of design Step 4

Step 5: Deposit respectively a layer of Cr and Ni to be used as heater, RFID antenna, and the conductors connected to the power supply. Then use mask #4 and PAEP to reserve the PR on the heater, RFID antenna, and the conductors connected to the power supply. Finally, remove the layers of Cr and Ni without PR protection. Remove the PR; the result is as shown in Fig. 6.

Step 6: Use mask #5 and PAEP to reserve the PR on the heater, and flash a layer of gold on Ni by electroless-plating. Thus the conductivity of the RFID antenna, and the conductors connected to the power supply can be very good. Besides, the performance of the soldering process on the pads for packaging would also be increased.

Step 7: Cover PR on the front side. Use mask #2 and PAEP to make the silicon dioxide layer uncovered by the PR at the grooved structure. Remove the dioxide layer, then the heater and the thermisters can be released and suspended over the grooved structure, the result is as shown in Fig. 7.

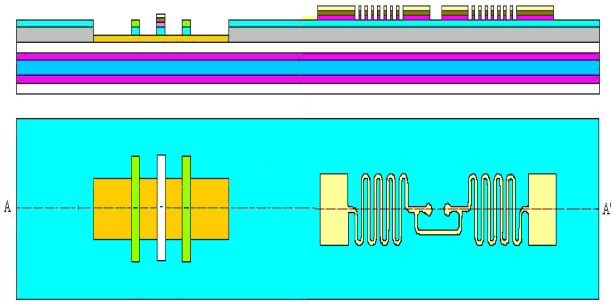

Fig. 6 Result of design Step 5

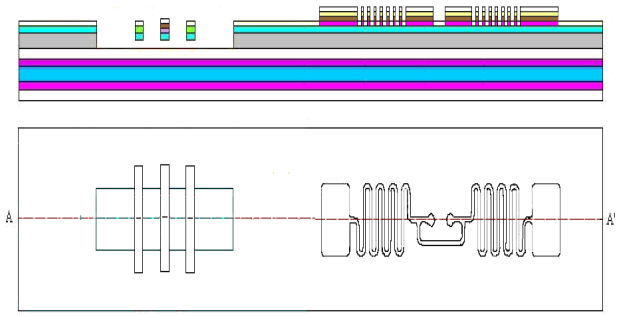

Fig. 7 Result of design Step 7

Step 8: Remove PR, and screen print plastic or polymer material around the inclinometer as dam bar, then put a cap on the dam bar and curing, before sealing it one can fill it with xenon gas. Finally, the chip with metal bump is flip chip bonded to the RFID feed terminal by thermal compression method, then the result is in Fig. 8.

Step 9: Put a socket to fix a battery on the substrate, the result is shown in Fig. 9, in which a full differential bridge circuit is applied. It should be noted that if the non-floating type structure without the cavity is needed, then one can skip the related steps to make the cavity in the steps 1-3 and 7.

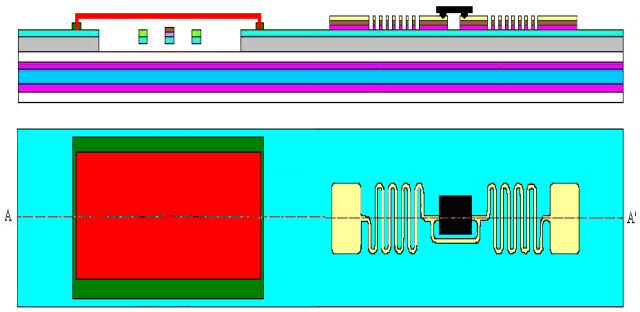

Fig. 8 Result of design Step 8

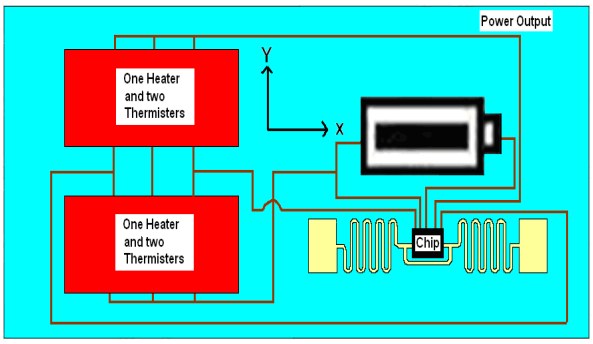

Fig. 9 Result of design Step 9

Simulation and Discussion

In this section the ESI-CFD$^+$ software package is applied for simulation [26-29]. Let the length and the floating height (H1) of thermisters and heater are 9mm and 1mm, respectively. The geometry definition of the inclinometer is as shown in Fig. 10(a), in which W1=0.5mm, W2=1mm, S=1.25mm and H=8.7mm. Besides, the temperature of the package boundaries and the heater are set as 300 and 400K, respectively. The chamber is filled with xenon or CO_2. The sensitivity curves (temperature differences of thermisters vs. tilt angles) are as shown in Fig. 10(b). Note that the sensitivity curves are in nonlinear manner by using either xenon or carbon dioxide gas. Thus the floating structure is not suitable; and we will apply the non-floating type as shown in Fig. 11 (where W1=0.1mm, W2=0.6mm, S=1.25mm, and H=9.9mm) in this paper the next. The sensitivity results for the non-floating structure with xenon and CO_2 gases by using hemispherical, hemi-cylindrical, and rectangular chambers are as shown in Figs. 12(a), (b) and (c), respectively. Note that the performances by using xenon are better than the one with CO_2. By the way if the inclination angle is 45°, the temperature profiles using xenon

and CO_2 gases for hemispherical, hemi-cylindrical, and rectangular chambers are respectively as shown in Figs. 13-15.

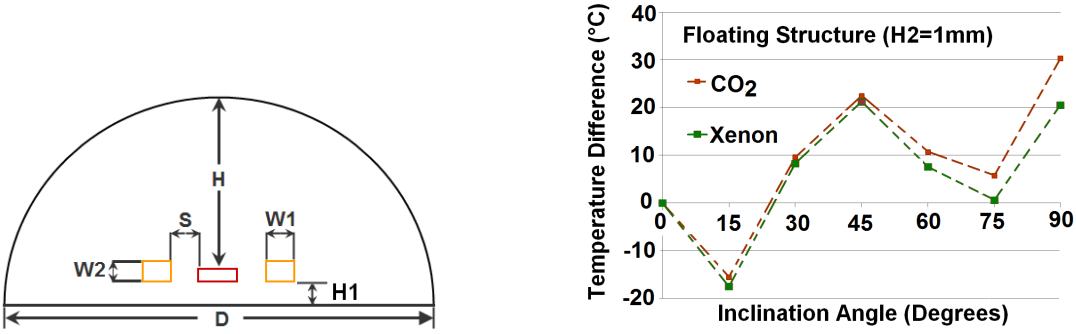

(a) Geometry. (b) Sensitivity curves with Xe CO_2 gases.

Fig. 10 Floating type inclinometer. (a) Geometry. (b) Sensitivity curves with Xe CO_2 gases.

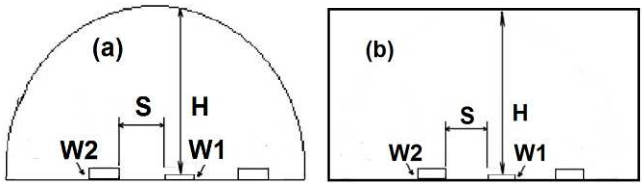

Fig. 11 Chambers of inclinometers. (a) Hemispherical and hemi-cylindrical. (b) Rectangular.

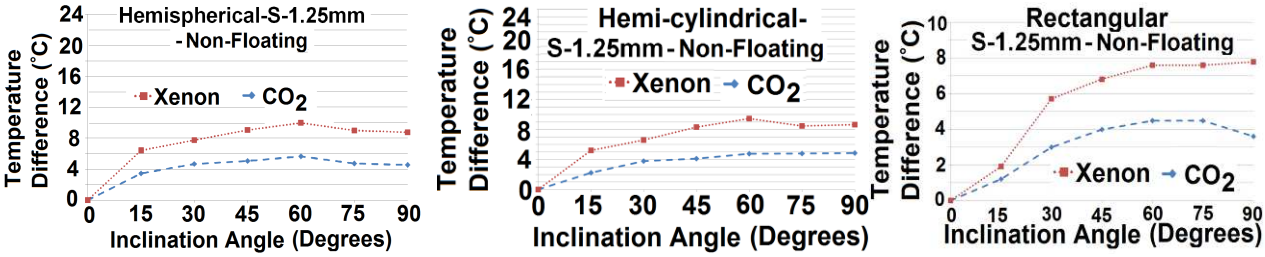

(a) (b)

Fig. 12 Sensitivity curve. (a)Hemispherical, (b) hemi-cylindrical and (c) rectangular chambers.

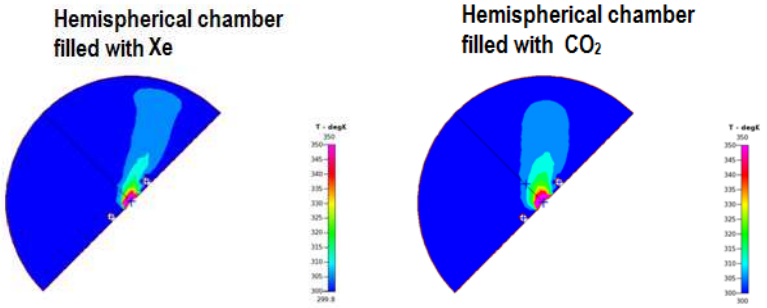

Fig. 13 Temperature profiles for hemispherical chamber with Xe and CO_2

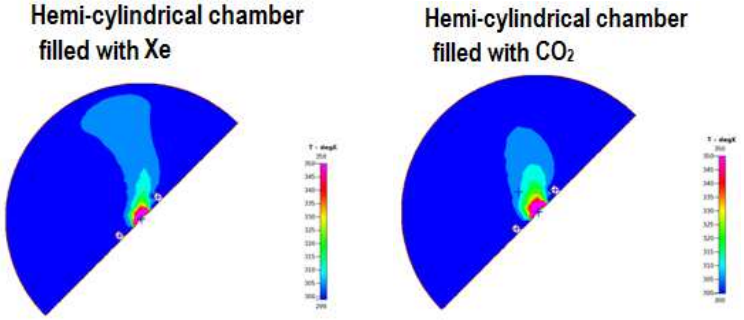

Fig. 14 Temperature profiles for hemi-cylindrical chamber with Xe and CO_2

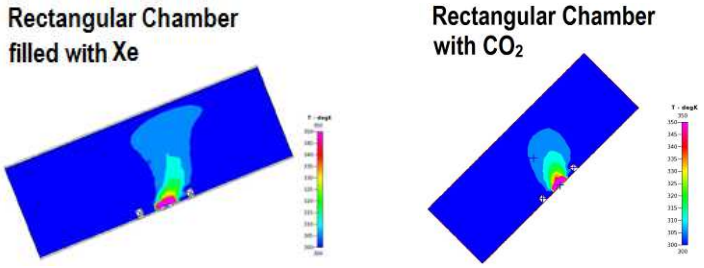

Fig. 15 Temperature profiles for rectangular chamber with Xe and CO_2

Note that the temperature profiles, so do the temperature gradient profiles by using Xe gas are extended to some larger spaces for all the kind of chambers, thus the sensor sensitivities are also larger. Note also that the temperature profiles by using hemispherical chamber with Xe and CO_2 are without distortion while the others will, so the sensitivities would be also larger by using hemispherical chamber. This can be proved for the results by using different chambers filled with CO_2 and Xe gases as shown in Figs. 16(a) and 16(b), respectively. Note that the performance by using the package with hemispherical chamber is better than the others for either gas. On the other hand, for comparison purpose if the inclination angle is still 45°, the velocity profiles using xenon and CO_2 gases for hemispherical, hemi-cylindrical, and rectangular chambers are respectively as shown in Figs. 17-19. Note that the velocity profiles by using Xe gas are also extended to some larger spaces for all the kind of chambers, thus the sensor response speed would be also quicker. Note also that the velocity profile by using hemi-cylindrical chamber with Xe and CO_2 are also larger than the others, so the sensor response speed would be the quickest by using hemi-cylindrical chamber with Xe.

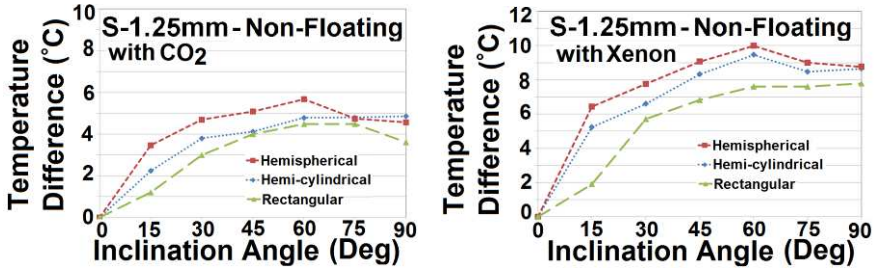

(a) (b)

Fig. 16 Sensitivity curves of non-floating structure filled with CO_2 and Xe gas

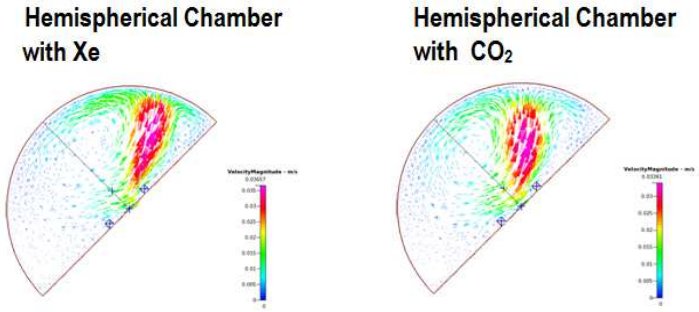

Fig. 17 Velocity profiles for hemispherical chamber with Xe and CO_2

This can also be proved for the results of step-input response by using hemispherical, hemi-cylindrical, and rectangular chambers as shown in Figs. 20-22, respectively. The results of response time (Tr) with xenon and CO_2 gases by using hemispherical, hemi-cylindrical, and rectangular chambers for tilting angles as 15, 30, 45, 60, 75, 90 degrees and the average response times (Tav) are also listed in TABLES I-III for comparison. Note that the response speed by using hemi-cylindrical chamber with xenon gas is the quickest; the average response time is 545μs, while the rectangular chamber filled with CO_2 is the slowest, and the average response time is 848μs.

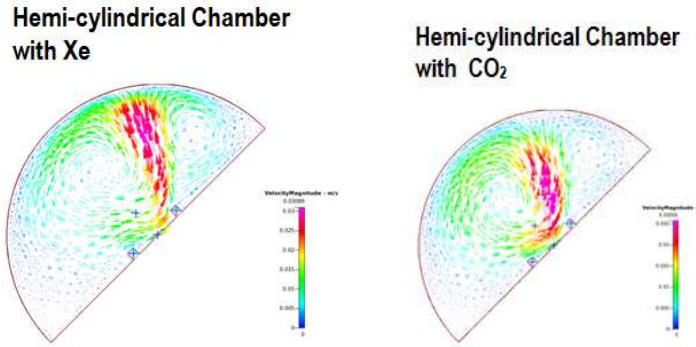

Fig. 18 Velocity profiles for hemi-cylindrical chamber with Xe and CO_2

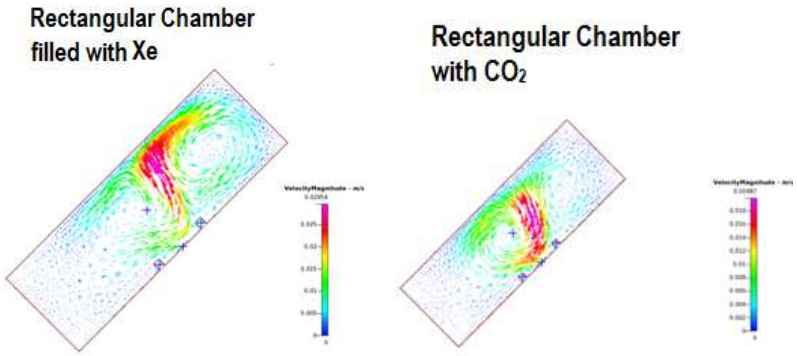

Fig. 19Velocity profiles for rectangular chamber with Xe and CO_2

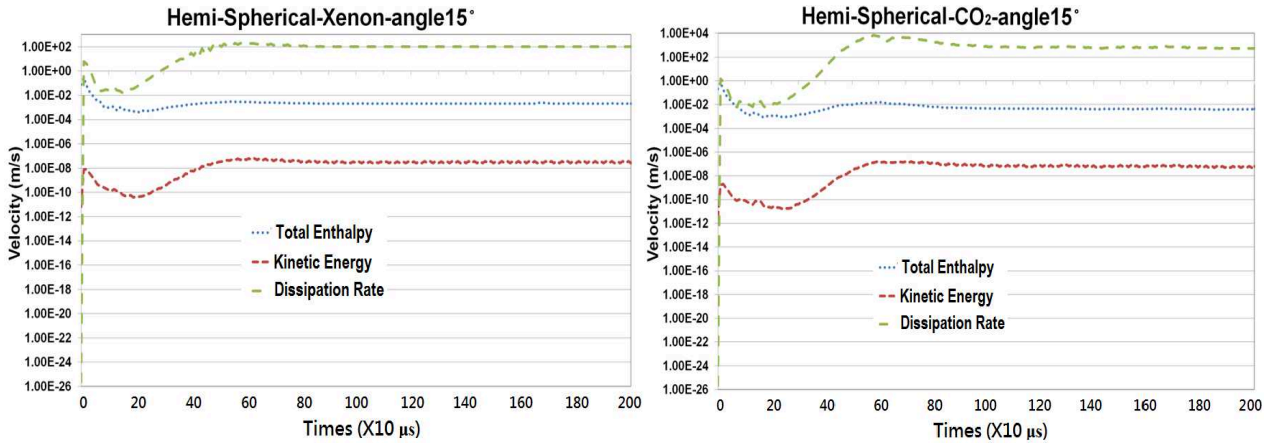

Fig. 20Step-input response by using non-floating structure for hemispherical chamber with xenon gas (a) and CO_2 gas (b) with the tilting angle is 15°

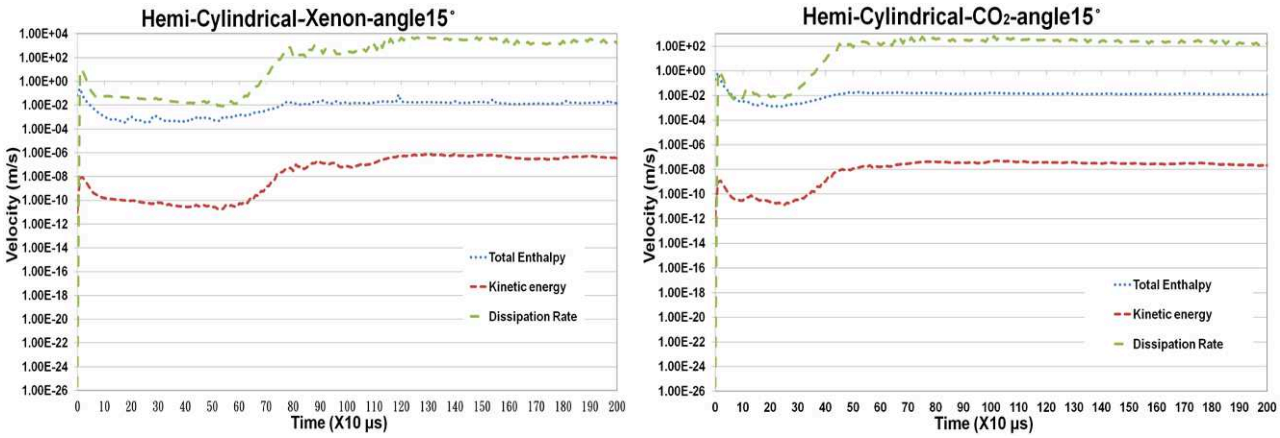

Fig. 21(a) Step-input response by using non-floating structure for hemi-cylindrical chamber with xenon gas (a) and CO_2 gas (b) with the tilting angle is 15°

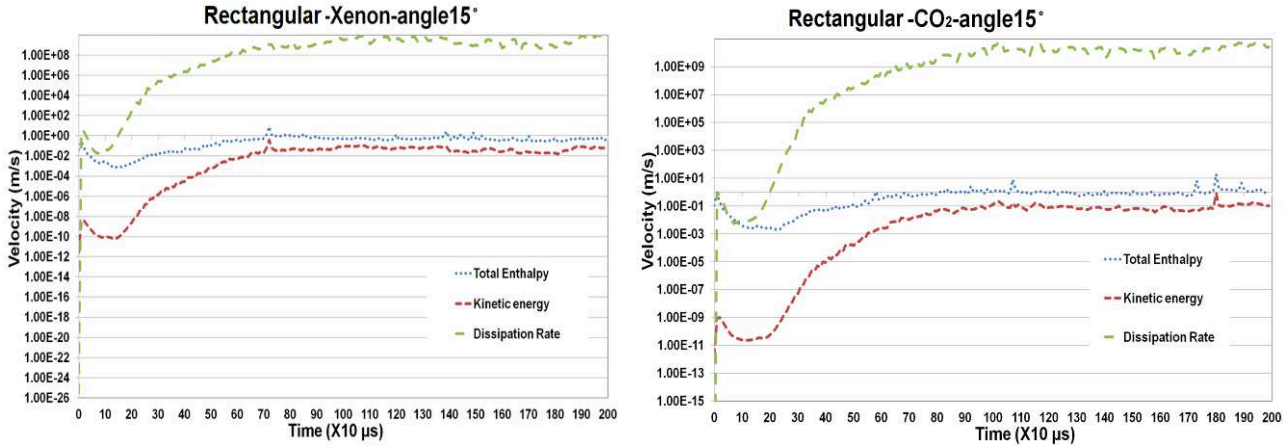

Fig. 22(a) Step-input response by using non-floating structure for rectangular chamber with xenon gas (a) and CO_2 gas (b) with the tilting angle is 15°

TABLE I

Step-input response times using hemispherical chamber filled with xenon and carbon dioxide

Tr (μs)	Tilting Angle (Degrees)						Tav
	15	30	45	60	75	90	(μs)
CO_2	730	670	750	630	640	970	748
Xenon	600	590	770	470	600	510	590

TABLE III

Step-input response times using hemi-cylindrical chamber filled with xenon and carbon dioxide

Tr (μs)	Tilting Angle (Degrees)						Tav
	15	30	45	60	75	90	(μs)
CO_2	640	710	640	610	740	800	690
Xenon	580	660	560	490	480	500	545

TABLE IIIII

Step-input response times using Rectangular chamber filled with xenon and carbon dioxide

Tr (μs)	Tilting Angle (Degrees)						Tav
	15	30	45	60	75	90	(μs)
CO_2	720	1030	730	970	970	670	848
Xenon	760	800	680	870	870	550	755

Conclusions

This research proposes a novel wireless RFID-based thermal convection type inclinometer. Four new ideas are presented. The first idea is to make the device on a flexible substrate, thus it can save more leakage energy to the environment. The second idea is to integrate both an inclinometer and a wireless RFID antenna on the same substrate for convenient to use. The third idea is to fill xenon gas in the chamber with hemi-spherical shape instead of the previous one with carbon dioxide and rectangular shape. Because the xenon gas would not produce oxidization effect to the heater, so it is more reliable. The fourth idea is to use a non-floating structure without a cavity in the substrate instead of the floating one. The new structure is easier to make and the cost is also much lower. The results by using floating structure are studied the first; but the sensitivity curves are not good. So the non-floating structure is applied in this paper. Note that the sensitivities for the proposed non-floating structure with xenon and CO_2 gases are better, and the one with xenon is better than using CO_2 by 70%. On the other hand, the response speed by using hemi-cylindrical chamber with xenon gas is the quickest, the average response time is 545μs, while the rectangular chamber filled with CO_2 is the slowest, and the average response time is 848μs.

Acknowledgements

This research was supported by National Science Council Taiwan, R.O.C. with contract NSC-101-2622-E-216-001-CC3, 101-2221-E-216-006-MY2, and 101-2221-E-216-019-.

References

[1] R. W. Lucky:Bell Syst. Tech. J. Vol. 44 (1965), p. 547

[2] S. P. Bingulac: in *Proc. 4th Annu. Allerton Conf. Circuits and Systems Theory*, (1994), p. 8

[3] G. R. Faulhaber, in: *IEEE Int. Conf. Communications,* (1995), p. 3

[4] W. D. Doyle: in *Proc. INTERMAG Conf.*, (1987), pp. 2.2-1

[5] S. Billata, H. Glosch, M Kunze, F. Hedrich, J. Frech, J. Auber, H. Sandmaier, W. Wimmer and W. Lang: Sensors and Actuators A: Physical Vol. 97-98 (2002), p. 125

[6] S. Billat, H. Glosch, M. Kunze, F. Hedrich, J. Frech, J. Auber, H. Sandmaier, W. Wimmer and W. Lang,: in *Proc. MEMS, Interlaken, Switzerland* (2001), p. 159

[7] M. A. Adams, P. Dolan, C. Marx and W. C. Hutton: Clinical Biomechanics Vol. 1 (1986), p. 130

[8] Frazão, R. Falate, J. L. Fabris, J. L. Santos, L. A. Ferreira and F. M. Araújo: Optics Letters Vol. 31 (2006), p. 2960

[9] A. G. Butler, D. G. Green and R. E. Nagle, U.S. patent 4 912 662. (1990)

[10] Ascia, S. Baglio and N. Savalli: Instrumentation and Measurement Vol. 56 (2007), p. 1114

[11] R. R. Baxter, S. Ohno, S. D. Hawley and D. M. Wilson: in *Proc. 12th International Conference on, 2003, Transducers, Solid-State Sensors, Actuators and Microsystems* Vol. 2 (2003), p. 1279

[12] A. M. Leung, J. Jones, E. Czyzewska, J. Chen and B. Woods: in *Proc. MEMS*, Anaheim, CA (1998), p. 627

[13] V. Milanovic, E. Bowen, Nim Tea, J. Suehle, B.Payne, M. Zaghloul and M. Gaitan: in *Proc. MEMS*, Anaheim CA, (1998), p. 487

[14] J. van Honschoten, J. van Baar, H. E. de Bree, T. Lammerink, G. Krijnen and J. M. Elwenspoek: Micromech. Microeng. Vol. 10 (2000), p. 250

[15] Y. Y. Cai, A. Dribinsky, G. J. O'Brien, G. P. Pucci, M. Varghese, U.S. Patent 7,862,229 B2. (2011)

[16] B. Alain, R. Alain, V. Bernard, G. Alain: European Patent E. Patent 1,550,874 B1. (2010)

[17] G. Daia, M. Li, X. P. He, L. M. Du, B. B. Shao and W. Su: Sensors and Actuators A: Physical Vol. 172 (2011), p. 369

[18] A. H. Ma and A. M. Leung: *IEEE* Sensors (2008) p. 1492

[19] J. Courteaud, P. Combette, N. Crespy, G. Cathebras and A. Giani: Sensors and Actuators A: Physical Vol. 141 (2008), p. 307

[20] S. Petra, E. F. Bernhard, F. Knut, S. Dagmar and H. Jan: Diagnostic Imaging and Testing, Vol. 21 (1996), p. 1332

[21] S. L. Cornbleet and N. B. Woolsey: Physical Therapy, Vol. 76 (1996), p. 850

[22] L. A. Rochaa, C. S. Silva, M. F. Cerqueira, J. F. Ribeiro, L. M. Goncalves, A. J. Pontes and J. C. Viana: Procedia Engineering, Vol. 25 (2011), p. 607